HHS Public Access

Author manuscript

J Nucl Med. Author manuscript; available in PMC 2015 August 22.

Published in final edited form as:

J Nucl Med. 2014 December ; 55(12): 2057–2063. doi:10.2967/jnumed.114.145896.

Introduction of an 8-Aminooctanoic Acid Linker Enhances the melanoma uptake of Tc-99m-labeled Lactam Bridge-Cyclized Alpha-MSH Peptide

Haixun Guo[1] and **Yubin Miao**[1,2,3]

[1]College of Pharmacy, University of New Mexico, Albuquerque, NM 87131, USA

[2]Cancer Research and Treatment Center, University of New Mexico, Albuquerque, NM 87131, USA

[3]Department of Dermatology, University of New Mexico, Albuquerque, NM 87131, USA

Abstract

The purpose of this study was to examine the effects of amino acid, hydrocarbon and polyethylene glycol (PEG) linkers on melanoma targeting and imaging properties of ^{99m}Tc-labeled lactam bridge-cyclized HYNIC-linker-Nle-CycMSH$_{hex}$ {hydrazinonicotinamide-linker-Nle-c[Asp-His-DPhe-Arg-Trp-Lys]-CONH$_2$} peptides.

Methods—four novel peptides {HYNIC-GGGNle-CycMSH$_{hex}$, HYNIC-GSGNle-CycMSH$_{hex}$, HYNIC-PEG$_2$Nle-CycMSH$_{hex}$ and HYNIC-AocNle-CycMSH$_{hex}$} were designed and synthesized. The melanocortin-1 (MC1) receptor binding affinities of the peptides were determined in B16/F1 melanoma cells. The biodistribution of ^{99m}Tc(EDDA)-HYNIC-GGGNle-CycMSH$_{hex}$, ^{99m}Tc(EDDA)-HYNIC-GSGNle-CycMSH$_{hex}$, ^{99m}Tc(EDDA)-HYNIC-PEG$_2$Nle-CycMSH$_{hex}$ and ^{99m}Tc(EDDA)-HYNIC-AocNle-CycMSH$_{hex}$ were determined in B16/F1 melanoma-bearing C57 mice at 2 h post-injection to select a lead peptide for further evaluation. The melanoma targeting and imaging properties of ^{99m}Tc(EDDA)-HYNIC-AocNle-CycMSH$_{hex}$ were further examined because of its high melanoma uptake.

Results—The IC$_{50}$ values of HYNIC-GGGNle-CycMSH$_{hex}$, HYNIC-GSGNle-CycMSH$_{hex}$, HYNIC-PEG$_2$Nle-CycMSH$_{hex}$, and HYNIC-AocNle-CycMSH$_{hex}$ were 0.7 ± 0.1, 0.8 ± 0.09, 0.4 ± 0.08, and 0.3 ± 0.06 nM in B16/F1 melanoma cells, respectively. Among these four ^{99m}Tc-labeled peptides, ^{99m}Tc(EDDA)-HYNIC-AocNle-CycMSH$_{hex}$ displayed the highest melanoma uptake (22.3 ± 1.72% ID/g) at 2 h post-injection. ^{99m}Tc(EDDA)-HYNIC-AocNle-CycMSH$_{hex}$ exhibited high tumor to normal organ uptake ratios except for the kidneys. The tumor/kidney uptake ratios of ^{99m}Tc(EDDA)-HYNIC-AocNle-CycMSH$_{hex}$ were 3.29, 3.63 and 6.78 at 2, 4 and 24 h post-injection. The melanoma lesions were clearly visualized by single photon emission computed tomography (SPECT)/CT using ^{99m}Tc(EDDA)-HYNIC-AocNle-CycMSH$_{hex}$ as an imaging probe at 2 h post-injection.

Corresponding Author: Yubin Miao, 2502 Marble NE, MSC09 5360, College of Pharmacy, University of New Mexico, Albuquerque, NM 87131, USA. Phone: (505) 925-4437; Fax: (505) 272-6749; ymiao@salud.unm.edu.
First Author: Haixun Guo, 2502 Marble NE, MSC09 5360, College of Pharmacy, University of New Mexico, Albuquerque, NM 87131. Phone: (505) 272-8034; Fax: (505) 272-6749; h0guo005@louisville.edu

Conclusion—High melanoma uptake and fast urinary clearance of ^{99m}Tc(EDDA)-HYNIC-AocNle-CycMSH$_{hex}$ highlighted its potential for metastatic melanoma detection in the future.

Keywords

Alpha-melanocyte stimulating hormone; ^{99m}Tc-labeled lactam bridge-cyclized peptide; melanoma imaging

INTRODUCTION

Over the past several years, radiolabeled lactam bridge-cyclized alpha-melanocyte stimulating hormone (α-MSH) peptides have become another new class of cyclic peptides for melanoma targeting (1–11). The lactam bridge-cyclized α-MSH peptides can bind to the melanocortin-1 (MC1) receptors with low nanomolar binding affinities. Thus, we have utilized the lactam bridge-cyclized α-MSH peptides to target diagnostic radionuclides (i.e. ^{111}In, ^{67}Ga and ^{64}Cu) to melanoma cells for imaging. Specifically, we attached DOTA (1,4,7,10-tetraazacyclododecane-1,4,7,10-tetraacetic acid) and NOTA (1,4,7-triazacyclononane-1,4,7-triacetic acid) to the MC1 receptor-targeting GGNle-CycMSH$_{hex}$ {Gly-Gly-Nle-c[Asp-His-DPhe-Arg-Trp-Lys]-CONH$_2$} peptide for radiolabeling of ^{111}In, ^{67}Ga and ^{64}Cu (9–11). The promising imaging results of ^{111}In-, ^{67}Ga- and ^{64}Cu-labeled DOTA/NOTA-GGNle-CycMSH$_{hex}$ highlighted their potential as imaging probes for single photon emission computed tomography (SPECT) and positron emission tomography (PET) imaging of melanoma (9–11).

Recently, building upon the success of ^{111}In-, ^{67}Ga- and ^{64}Cu-labeled DOTA/NOTA-GGNle-CycMSH$_{hex}$, we have further developed new ^{99m}Tc-labeled lactam bridge-cyclized α-MSH peptides to take advantage of the ideal imaging properties of ^{99m}Tc (140-keV γ-photon and 6 h half-life) and its wide application in nuclear medicine. Specifically, we replaced DOTA/NOTA with bifunctional metal chelators such as mercaptoacetyltriglycine (MAG$_3$), Ac-Cys-Gly-Gly-Gly (AcCG$_3$) and hydrazinonicotinamide (HYNIC) for ^{99m}Tc radiolabeling (12). HYNIC-GGNle-CycMSH$_{hex}$ was readily radiolabeled with ^{99m}Tc in Ethylenediaminediacetic acid (EDDA)/Tricine solution. Interestingly, ^{99m}Tc(EDDA)-HYNIC-GGNle-CycMSH$_{hex}$ exhibited higher melanoma uptake and faster urinary clearance than ^{99m}Tc-MAG$_3$-GGNle-CycMSH$_{hex}$ and ^{99m}Tc-AcCG$_3$-GGNle-CycMSH$_{hex}$ in B16/F1 melanoma-bearing C57 mice. The B16/F1 melanoma lesions were clearly visualized by SPECT/CT using ^{99m}Tc(EDDA)-HYNIC-GGNle-CycMSH$_{hex}$ as an imaging probe (12).

In our previous report, the introduction of -GlyGly- amino acid linker resulted in lower renal and liver uptake of ^{111}In-DOTA-GGNle-CycMSH$_{hex}$ as compared to ^{111}In-DOTA-Nle-CycMSH$_{hex}$ (9). Meanwhile, hydrocarbon, amino acid and PEG linkers displayed profound favorable effects in the receptor binding affinities and pharmacokinetics of radiolabeled bombesin (13–17), RGD (18–21) and α-MSH peptides (1, 3). Thus, we were interested in examining how the amino acid, hydrocarbon and PEG linkers affect the melanoma targeting and pharmacokinetic properties of ^{99m}Tc(EDDA)-HYNIC-linker-Nle-CycMSH$_{hex}$ peptides. Building on the HYNIC-GGNle-CycMSH$_{hex}$ construct, we designed four novel peptides with different amino acid, hydrocarbon and PEG linkers in this study. Two neutral -

GlyGlyGly- (GGG) and -GlySerGly- (GSG) amino acid linkers, one -Aoc- (8-aminooctanoic acid) hydrocarbon linker and one -PEG_2- linker were inserted between the HYNIC and Nle-$CycMSH_{hex}$ to generate HYNIC-GGGNle-$CycMSH_{hex}$, HYNIC-GSGNle-$CycMSH_{hex}$, HYNIC-AocNle-$CycMSH_{hex}$, and HYNIC-PEG_2Nle-$CycMSH_{hex}$ peptides. The MC1 receptor binding affinities of these four peptides were determined in B16/F1 melanoma cells. Then, we radiolabeled the peptides with ^{99m}Tc using the EDDA/Tricine solution. We examined the biodistribution of ^{99m}Tc(EDDA)-HYNIC-GGGNle-$CycMSH_{hex}$, ^{99m}Tc(EDDA)-HYNIC-GSGNle-$CycMSH_{hex}$, ^{99m}Tc(EDDA)-HYNIC-AocNle-$CycMSH_{hex}$, ^{99m}Tc(EDDA)-HYNIC-PEG_2Nle-$CycMSH_{hex}$ at 2 h post-injection to select a lead ^{99m}Tc-peptide for further evaluation. ^{99m}Tc(EDDA)-HYNIC-AocNle-$CycMSH_{hex}$ displayed the highest melanoma uptake at 2 h post-injection. Therefore, we further determined the biodistribution of ^{99m}Tc(EDDA)-HYNIC-AocNle-$CycMSH_{hex}$ and its property for molecular imaging in B16/F1 melanoma-bearing C57 mice in this study.

MATERIALS AND METHODS

Chemicals and Reagents

Amino acid and resin were purchased from Advanced ChemTech Inc. (Louisville, KY) and Novabiochem (San Diego, CA). Boc-HYNIC was purchased from VWR International, Inc. (Albuquerque, NM) for peptide synthesis. ^{125}I-Tyr^2-[Nle^4, D-Phe^7]-α-MSH {^{125}I-(Tyr^2)-NDP-MSH} was obtained from PerkinElmer, Inc. (Waltham, MA) for receptor binding assay. $^{99m}TcO_4^-$ was purchased from Cardinal Health (Albuquerque, NM) for peptide radiolabeling. All other chemicals used in this study were purchased from Thermo Fischer Scientific (Waltham, MA) and used without further purification. B16/F1 murine melanoma cells were obtained from American Type Culture Collection (Manassas, VA).

Peptide Synthesis and Receptor Binding Assay

HYNIC-GGGNle-$CycMSH_{hex}$, HYNIC-GSGNle-$CycMSH_{hex}$, HYNIC-AocNle-$CycMSH_{hex}$ and HYNIC-PEG_2Nle-$CycMSH_{hex}$ were synthesized using fluorenylmethyloxy carbonyl (Fmoc) chemistry, purified by reverse phase-high performance liquid chromatography (RP-HPLC) and characterized by liquid chromatography-mass spectrometry (LC-MS). Generally, 70 μmol of resin, 210 μmol of each Fmoc-protected amino acid and 210 μmol of Boc-HYNIC were used for the synthesis. Briefly, the intermediate scaffolds of HYNIC(Boc)-[Gly-Gly-Gly/Gly-Ser(Trt)-Gly/Aoc/PEG_2]-Nle-Asp(O-2-PhiPr)-His(Trt)-DPhe-Arg(Pbf)-Trp(Boc)-Lys(Dde) were synthesized on H_2N-Sieber amide resin by an Advanced ChemTech multiple-peptide synthesizer (Louisville, KY). The protecting group of Dde was removed by 2% hydrazine for peptide cyclization. The protecting group of 2-phenylisopropyl was removed and the protected peptide was cleaved from the resin treating with a mixture of 2.5% of trifluoroacetic acid (TFA) and 5% of triisopropylsilane. Each protected peptide was cyclized by coupling the carboxylic group from the Asp with the epsilon amino group from the Lys. The cyclization reaction was achieved by an overnight reaction in dimethylformamide (DMF) using benzotriazole-1-yl-oxy-tris-pyrrolidino-phosphonium-hexafluorophosphate (PyBOP) as a coupling agent in the presence of N,N-diisopropylethylamine (DIPEA). Then, each protected cyclic peptide was dissolved in H_2O/CH_3CN (50:50) and lyophilized to remove the reagents. The protecting

groups were totally removed by treating with a mixture of trifluoroacetic acid (TFA), thioanisole, phenol, water, ethanedithiol and triisopropylsilane (87.5:2.5:2.5:2.5:2.5:2.5) for 2 h at room temperature (25 °C). Each peptide was precipitated and washed with ice-cold ether four times, purified by reverse phase-high performance liquid chromatography (RP-HPLC) and characterized by LC-mass spectroscopy (LC-MS). The MC1 receptor binding affinities (IC_{50} values) of HYNIC-GGGNle-CycMSH$_{hex}$, HYNIC-GSGNle-CycMSH$_{hex}$, HYNIC-AocNle-CycMSH$_{hex}$ and HYNIC-PEG$_2$Nle-CycMSH$_{hex}$ were determined in B16/F1 melanoma cells by *in vitro* competitive receptor binding assay according to our published procedure (9).

Peptide Radiolabeling with ^{99m}Tc

^{99m}Tc(EDDA)-HYNIC-GGGNle-CycMSH$_{hex}$, ^{99m}Tc(EDDA)-HYNIC-GSGNle-CycMSH$_{hex}$, ^{99m}Tc(EDDA)-HYNIC-AocNle-CycMSH$_{hex}$, ^{99m}Tc(EDDA)-HYNIC-PEG$_2$Nle-CycMSH$_{hex}$ were prepared according to our published procedure (12). Briefly, 50 μL of $^{99m}TcO_4^-$ (37–74 MBq), 10 μL of 1 mg/mL $SnCl_2$ in 0.1 N HCl solution, 200 μL of a mixture of 5 mg/mL of EDDA and 25 mg/mL of Tricine aqueous solution and 10 μL of 1 mg/mL each peptide aqueous solution were added into 400 μL of 0.5 M NH_4OAc (pH 5.44) in a reaction vial and incubated at 95°C for 30 min. Each radiolabeled peptide was purified to a single species by Waters RP-HPLC on a Grace Vydac C-18 reverse phase analytic column using a 20-min gradient of 20–30% acetonitrile in 20 mM HCl aqueous solution at a flow rate of 1 mL/min. The purified peptide was purged with N_2 gas for 20 min to remove the acetonitrile. The pH of the final solution was adjusted to 5 with 0.1 N NaOH and normal saline for animal studies.

Biodistribution Studies

All animal studies were conducted in compliance with Institutional Animal Care and Use Committee approval. In an attempt to select a lead ^{99m}Tc-peptide for further evaluation, the biodistribution of ^{99m}Tc(EDDA)-HYNIC-GGGNle-CycMSH$_{hex}$, ^{99m}Tc(EDDA)-HYNIC-GSGNle-CycMSH$_{hex}$, ^{99m}Tc(EDDA)-HYNIC-AocNle-CycMSH$_{hex}$, and ^{99m}Tc(EDDA)-HYNIC-PEG$_2$Nle-CycMSH$_{hex}$ were examined in B16/F1 melanoma-bearing C57 female mice (Harlan, Indianapolis, IN) at 2 h post-injection, respectively. The C57 mice were subcutaneously inoculated with 1×10^6 B16/F1 cells on the right flank for each mouse to generate B16/F1 tumors. The weights of tumors reached approximately 0.2 g 10 days post cell inoculation. Each melanoma-bearing mouse was injected with 0.037 MBq of ^{99m}Tc(EDDA)-HYNIC-GGGNle-CycMSH$_{hex}$, ^{99m}Tc(EDDA)-HYNIC-GSGNle-CycMSH$_{hex}$, ^{99m}Tc(EDDA)-HYNIC-AocNle-CycMSH$_{hex}$ or ^{99m}Tc(EDDA)-HYNIC-PEG$_2$Nle-CycMSH$_{hex}$ via the tail vein. Groups of 5 mice were sacrificed at 2 h post-injection, tumor and organs of interest were harvested, weighed and counted in a Wallace 1480 automated gamma counter (PerkinElmer). Meanwhile, intestines and urine were collected and counted to evaluate the clearance pathway of each ^{99m}Tc-peptide. Blood was taken as 6.5% of the body weight.

^{99m}Tc(EDDA)-HYNIC-AocNle-CycMSH$_{hex}$ displayed higher melanoma uptake than the other three ^{99m}Tc-peptides. Therefore, the biodistribution of ^{99m}Tc(EDDA)-HYNIC-GGNle-CycMSH$_{hex}$ at 0.5, 4 and 24 h post-injection was determined in B16/F1 melanoma-

bearing C57 female mice. B16/F1 melanoma-bearing mice were generated as described above. Each melanoma-bearing mouse was injected with 0.037 MBq of ^{99m}Tc(EDDA)-HYNIC-AocNle-CycMSH$_{hex}$ via the tail vein. Groups of 5 mice were sacrificed at 0.5, 4 and 24 h post-injection, and tumors and organs of interest were harvested, weighed and counted. Blood was taken as 6.5% of the body weight. The tumor uptake specificity of ^{99m}Tc(EDDA)-HYNIC-AocNle-CycMSH$_{hex}$ was determined by co-injecting 10 μg (6.07 nmol) of unlabeled NDP-MSH peptide at 2 h post-injection. To examine whether *L*-lysine co-injection could decrease the renal uptake, a group of 5 mice was injected with a mixture of 12 mg of *L*-lysine and 0.037 MBq of ^{99m}Tc(EDDA)-HYNIC-AocNle-CycMSH$_{hex}$. The mice were sacrificed at 2 h post-injection and the tumors and organs of interest were harvested, weighed and counted.

Melanoma Imaging of ^{99m}Tc(EDDA)-HYNIC-AocNle-CycMSH$_{hex}$

Approximately 9.3 MBq of ^{99m}Tc(EDDA)-HYNIC-AocNle-CycMSH$_{hex}$ was injected in a B16/F1 melanoma-bearing C57 mouse for melanoma imaging. The mouse was euthanized at 2 h post-injection for small animal SPECT/CT (Nano-SPECT/CT®, Bioscan) imaging. The 9-min CT imaging was immediately followed by the whole-body SPECT scan. The SPECT scans of 24 projections were acquired. Reconstructed SPECT and CT data were visualized and co-registered using InVivoScope (Bioscan, Washington DC).

Statistical Analysis

Statistical analysis was performed using the Student's t-test for unpaired data. A 95% confidence level was chosen to determine the significance of difference in tumor and renal uptake of ^{99m}Tc(EDDA)-HYNIC-AocNle-CycMSH$_{hex}$ with/without NDP-MSH co-injection, as well as the significance of difference in tumor and renal uptake of ^{99m}Tc(EDDA)-HYNIC-AocNle-CycMSH$_{hex}$ with/without *L*-lysine co-injection in the biodistribution studies described above. The differences at the 95% confidence level ($p<0.05$) were considered significant.

RESULTS

New HYNIC-GGGNle-CycMSH$_{hex}$, HYNIC-GSGNle-CycMSH$_{hex}$, HYNIC-AocNle-CycMSH$_{hex}$ and HYNIC-PEG$_2$Nle-CycMSH$_{hex}$ were synthesized and purified by RP-HPLC. All four peptides displayed greater than 95% purity after HPLC purification. The identities of HYNIC-GGGNle-CycMSH$_{hex}$, HYNIC-GSGNle-CycMSH$_{hex}$, HYNIC-AocNle-CycMSH$_{hex}$ and HYNIC-PEG$_2$Nle-CycMSH$_{hex}$ were confirmed by electrospray ionization mass spectrometry. The calculated and found molecular weights of HYNIC-GGGNle-CycMSH$_{hex}$, HYNIC-GSGNle-CycMSH$_{hex}$, HYNIC-AocNle-CycMSH$_{hex}$, and HYNIC-PEG$_2$Nle-CycMSH$_{hex}$ are presented in Table 1. The found molecular weights matched the calculated molecular weights. The schematic structures of HYNIC-GGGNle-CycMSH$_{hex}$, HYNIC-GSGNle-CycMSH$_{hex}$, HYNIC-AocNle-CycMSH$_{hex}$, and HYNIC-PEG$_2$Nle-CycMSH$_{hex}$ are shown in Figure 1. The IC$_{50}$ values of HYNIC-GGGNle-CycMSH$_{hex}$, HYNIC-GSGNle-CycMSH$_{hex}$, HYNIC-AocNle-CycMSH$_{hex}$, and HYNIC-PEG$_2$Nle-CycMSH$_{hex}$ were 0.7 ± 0.1, 0.8 ± 0.09, 0.4 ± 0.08 and 0.3 ± 0.06 nM in B16/F1 melanoma cells, respectively (Figure 2).

HYNIC-GGGNle-CycMSH$_{hex}$, HYNIC-GSGNle-CycMSH$_{hex}$, HYNIC-AocNle-CycMSH$_{hex}$, and HYNIC-PEG$_2$Nle-CycMSH$_{hex}$ were readily labeled with ^{99m}Tc with greater than 95% radiolabeling yields in EDDA/Tricine solution. Each radiolabeled peptide was completely separated from its excess non-labeled peptide by RP-HPLC. All ^{99m}Tc-peptides displayed greater than 98% radiochemical purities after HPLC purification. The retention times of ^{99m}Tc(EDDA)-HYNIC-GGGNle-CycMSH$_{hex}$, ^{99m}Tc(EDDA)-HYNIC-GSGNle-CycMSH$_{hex}$, ^{99m}Tc(EDDA)-HYNIC-AocNle-CycMSH$_{hex}$ and ^{99m}Tc(EDDA)-HYNIC-PEG$_2$Nle-CycMSH$_{hex}$ were 12.7, 10.6, 24.0 and 16.8 min, respectively. The retention times of HYNIC-GGGNle-CycMSH$_{hex}$, HYNIC-GSGNle-CycMSH$_{hex}$, HYNIC-AocNle-CycMSH$_{hex}$ and HYNIC-PEG$_2$Nle-CycMSH$_{hex}$ were 9.5, 8.3, 17.9 and 14.6 min, respectively.

The melanoma targeting and pharmacokinetic properties of ^{99m}Tc(EDDA)-HYNIC-GGGNle-CycMSH$_{hex}$, ^{99m}Tc(EDDA)-HYNIC-GSGNle-CycMSH$_{hex}$, ^{99m}Tc(EDDA)-HYNIC-AocNle-CycMSH$_{hex}$ and ^{99m}Tc(EDDA)-HYNIC-PEG$_2$Nle-CycMSH$_{hex}$ were determined in B16/F1 melanoma-bearing mice at 2 h post-injection to select a lead radiolabeled peptide for further evaluation. The biodistribution results of these four ^{99m}Tc-peptides are shown in Table 2. ^{99m}Tc(EDDA)-HYNIC-GGGNle-CycMSH$_{hex}$ and ^{99m}Tc(EDDA)-HYNIC-GSGNle-CycMSH$_{hex}$ displayed substantial tumor uptake of 9.78 ± 3.40 %ID/g and 7.41 ± 4.26 %ID/g at 2 h post-injection. ^{99m}Tc(EDDA)-HYNIC-PEG$_2$Nle-CycMSH$_{hex}$ showed higher tumor uptake of 14.32 ± 2.82 %ID/g at 2 h post-injection. ^{99m}Tc(EDDA)-HYNIC-AocNle-CycMSH$_{hex}$ exhibited the highest tumor uptake of 22.3 ± 1.72 %ID/g at 2 h post-injection among all four ^{99m}Tc-peptides. All ^{99m}Tc-peptides showed fast urinary clearance, approximately 89–94% of injected activities clear out of the body at 2 h post-injection. The accumulation in normal organs was lower than 0.81 %ID/g at 2 h post-injection for all four ^{99m}Tc-peptides except for kidneys. The renal uptake values were in a similar range (3.9–6.5 %ID/g at 2 h post-injection) for all four ^{99m}Tc-peptides. Thus, we selected ^{99m}Tc(EDDA)-HYNIC-AocNle-CycMSH$_{hex}$ as a lead peptide to further examine its full biodistribution and melanoma imaging properties.

The full biodistribution results of ^{99m}Tc(EDDA)-HYNIC-AocNle-CycMSH$_{hex}$ are presented in Table 3. ^{99m}Tc(EDDA)-HYNIC-AocNle-CycMSH$_{hex}$ displayed high tumor uptake and prolonged tumor retention in B16/F1 melanoma-bearing C57 mice. The tumor uptake was 23.44 ± 3.37 %ID/g and 22.8 ± 1.71 %ID/g at 0.5 and 2 h post-injection, respectively. As compared to the tumor uptake at 2 h post-injection, 97.2% of the radioactivity remained in tumor at 4 h post-injection. In melanoma uptake blocking study, co-injection of NDP-MSH blocked 94.5% of tumor uptake ($p<0.05$) at 2 h post-injection, demonstrating that the tumor uptake was MC1 receptor-medicated. Normal organ uptake of ^{99m}Tc(EDDA)-HYNIC-AocNle-CycMSH$_{hex}$ was lower than 1.26 %ID/g in normal tissues except for kidneys at 2, 4 and 24 h post-injection. High tumor/blood and high tumor/normal organ uptake ratios were achieved as early as 0.5 h post-injection. As the major excretion pathway of ^{99m}Tc(EDDA)-HYNIC-AocNle-CycMSH$_{hex}$, the kidney uptake was 19.65 ± 7.36% ID/g at 0.5 h post-injection and decreased to 1.05± 0.07% ID/g at 24 h post-injection. The tumor/kidney uptake ratios of ^{99m}Tc(EDDA)-HYNIC-AocNle-CycMSH$_{hex}$ were 3.29, 3.63 and 6.78 at 2, 4 and 24 h post-injection. Co-injection of NDP-MSH didn't reduce the renal uptake of the ^{99m}Tc(EDDA)-HYNIC-AocNle-CycMSH$_{hex}$ activity at 2 h

post-injection, indicating that the renal uptake was not MC1 receptor-mediated. Meanwhile, *L*-lysine co-injection decreased 33% of the renal uptake ($p<0.05$) without affecting the tumor uptake. Moreover, ^{99m}Tc(EDDA)-HYNIC-AocNle-CycMSH$_{hex}$ exhibited rapid urinary excretion. Approximately 88% of the activity cleared out of the body at 2 h post-injection. The representative whole-body, coronal and transversal SPECT/CT images are presented in Figure 3. The melanoma lesions were clearly visualized by SPECT/CT using ^{99m}Tc(EDDA)-HYNIC-AocNle-CycMSH$_{hex}$ as an imaging probe at 2 h post-injection. ^{99m}Tc(EDDA)-HYNIC-AocNle-CycMSH$_{hex}$ exhibited high tumor to normal organ uptake ratios except for the kidneys, which was consistent with the biodistribution results.

DISCUSSION

Over the past several years, several research groups have reported ^{99m}Tc-labeled α-MSH peptides (2, 5, 8, 12, 22–24) to target the melanocortin-1 (MC1) receptors for melanoma imaging taking advantage of the ideal imaging properties of ^{99m}Tc. Recently, we have developed a novel class of radiolabeled lactam bridge-cyclized α-MSH peptides to target MC1 receptors for melanoma imaging. Specifically, we have radiolabeled HYNIC/DOTA/NOTA-GGNle-CycMSH$_{hex}$ with ^{99m}Tc, ^{111}In, ^{67}Ga and ^{64}Cu for SPECT and PET imaging of melanoma (9–12). In our previous report, we found that the Nle-CycMSH$_{hex}$ moiety was critical for nanomolar MC1 receptor binding affinity of the DOTA-conjugated peptide (9). Introduction of a -GlyGlu- linker between the Nle and CycMSH$_{hex}$ moiety sacrificed the receptor binging affinity by 485-fold (9). Meanwhile, HYNIC was a better chelator for ^{99m}Tc than other N_3S chelators in terms of melanoma uptake and urinary clearance (12). In this study, we managed to examine the effects of amino acid, hydrocarbon and PEG linkers on the melanoma targeting properties of ^{99m}Tc-labeled lactam bridge-cyclized α-MSH peptide. Specifically, we introduced -GGG-, -GSG-, -Aoc- and -PEG_2- linkers between the HYNIC and Nle-CycMSH$_{hex}$ moiety to generate new HYNIC-GGGNle-CycMSH$_{hex}$, HYNIC-GSGNle-CycMSH$_{hex}$, HYNIC-AocNle-CycMSH$_{hex}$, and HYNIC-PEG_2Nle-CycMSH$_{hex}$ peptides. It is worthwhile to note that the lengths of -GGG-, -GSG-, -Aoc- and -PEG_2- linkers are same, eliminating the effect of the linker length on the melanoma targeting properties.

The introduction of -GGG-, -GSG-, -Aoc- and -PEG_2- linkers retained low nanomolar MC1 receptor binding affinities of the peptides. The IC_{50} was 0.7 ± 0.1 nM for HYNIC-GGGNle-CycMSH$_{hex}$, 0.8 ± 0.09 nM for HYNIC-GGGNle-CycMSH$_{hex}$, 0.4 ± 0.08 nM for HYNIC-AocNle-CycMSH$_{hex}$, and 0.3 ± 0.06 nM for HYNIC-PEG_2Nle-CycMSH$_{hex}$ (Table 1), respectively. Furthermore, we radiolabeled these four peptides with ^{99m}Tc and determined their biodistribution properties in B16/F1 melanoma-bearing C57 mice at 2 h post-injection to examine how the amino acid, hydrocarbon and PEG linkers affected their melanoma targeting and pharmacokinetic properties. Despite the slightly difference in receptor binding affinity among HYNIC-GGGNle-CycMSH$_{hex}$, HYNIC-GSGNle-CycMSH$_{hex}$, HYNIC-AocNle-CycMSH$_{hex}$, and HYNIC-PEG_2Nle-CycMSH$_{hex}$ peptides, we observed dramatic difference in melanoma uptake among these four ^{99m}Tc-peptides. As shown in Table 2, ^{99m}Tc(EDDA)-HYNIC-AcoNle-CycMSH$_{hex}$ exhibited the highest tumor uptake among these four ^{99m}Tc-peptides at 2 h post-injection in B16/F1 melanoma-bearing C57 mice. The

tumor uptake ^{99m}Tc(EDDA)-HYNIC-AcoNle-CycMSH$_{hex}$ was 2.3, 3.0 and 1.6 times the tumor uptake of ^{99m}Tc(EDDA)-HYNIC-GGGNle-CycMSH$_{hex}$, ^{99m}Tc(EDDA)-HYNIC-GSGNle-CycMSH$_{hex}$ ^{99m}Tc(EDDA)-HYNIC-PEG$_2$Nle-CycMSH$_{hex}$ at 2 h post-injection, respectively. Thus, we further examined the full biodistribution and melanoma imaging properties of ^{99m}Tc(EDDA)-HYNIC-AocNle-CycMSH$_{hex}$.

As shown in Table 3, ^{99m}Tc(EDDA)-HYNIC-AocNle-CycMSH$_{hex}$ displayed high tumor uptake and prolonged tumor retention in B16/F1 melanoma-bearing C57 mice. The tumor uptake was 23.44 ± 3.37 %ID/g and 22.8 ± 1.71 %ID/g at 0.5 and 2 h post-injection, respectively. In comparison with the tumor uptake at 2 h post-injection, 97.2% of the radioactivity remained in tumor at 4 h post-injection. Co-injection of NDP-MSH blocked 94.5% of tumor uptake ($p<0.05$) without affecting the renal uptake at 2 h post-injection, demonstrating that the tumor uptake was MC1 receptor-medicated and the renal uptake was non-specific. ^{99m}Tc(EDDA)-HYNIC-AocNle-CycMSH$_{hex}$ exhibited low accumulation in normal organs and a rapid urinary excretion, resulting in high tumor to normal organ uptake ratios. As we anticipated, the B16/F1 melanoma lesions were clearly visualized by SPECT/CT using ^{99m}Tc(EDDA)-HYNIC-AocNle-CycMSH$_{hex}$ as an imaging probe.

Recently, it has been reported that one more carboxylic group resulted in a dramatic decrease in the renal and liver uptake of ^{99m}Tc(CO)$_3$-labeled lactam bridge-cyclized α-MSH peptides (8). Accordingly, we anticipate that the introduction of a negatively-charged amino acid would further reduce the renal uptake. In this study, *L*-lysine co-injection decreased 33% of the renal uptake ($p<0.05$) without affecting the tumor uptake, indicating that the overall positive charge of ^{99m}Tc(EDDA)-HYNIC-AocNle-CycMSH$_{hex}$ contributed to its non-specific renal uptake. As shown in Figure 1, there was a positively-charged side chain in Arg^8, which contributed the overall positive charge of ^{99m}Tc(EDDA)-HYNIC-AocNle-CycMSH$_{hex}$. However, the Arg^8 is critical for MC1 receptor binding. Thus, it would be better to introduce a negatively-charged amino acid between the HYNIC and Aoc linker to decrease the overall charge of the peptide.

At the present time, ^{99m}Tc(EDDA)-HYNIC-GGNle-CycMSH$_{hex}$ and ^{99m}Tc-(Arg^{11})CCMSH displayed comparable high melanoma uptake (13.23 ± 2.35 vs. 11.16 ± 1.77 %ID/g) at 4 h post-injection. Remarkably, the tumor uptake of ^{99m}Tc(EDDA)-HYNIC-AocNle-CycMSH$_{hex}$ was 1.7 times the tumor uptake of ^{99m}Tc(EDDA)-HYNIC-GGNle-CycMSH$_{hex}$ at 4 h post-injection. Meanwhile, ^{99m}Tc(EDDA)-HYNIC-AocNle-CycMSH$_{hex}$ displayed higher tumor-to-kidney uptake ratios than ^{99m}Tc(EDDA)-HYNIC-GGNle-CycMSH$_{hex}$ at 2, 4 and 24 h post-injection. The tumor-to-kidney uptake ratio of ^{99m}Tc(EDDA)-HYNIC-AocNle-CycMSH$_{hex}$ was 1.8, 1.5, 1.9 times the tumor-to-kidney uptake ratio of ^{99m}Tc(EDDA)-HYNIC-GGNle-CycMSH$_{hex}$ at 2, 4 and 24 h post-injection. Overall, the properties of high melanoma uptake and fast urinary clearance of ^{99m}Tc(EDDA)-HYNIC-AocNle-CycMSH$_{hex}$ highlighted its potential as an imaging probe for metastatic melanoma detection in the future.

CONCLUSIONS

The biodistribution of ^{99m}Tc(EDDA)-HYNIC-GGGNle-CycMSH$_{hex}$, ^{99m}Tc(EDDA)-HYNIC-GSGNle-CycMSH$_{hex}$, ^{99m}Tc(EDDA)-HYNIC-AocNle-CycMSH$_{hex}$ and ^{99m}Tc(EDDA)-HYNIC-PEG$_2$Nle-CycMSH$_{hex}$ were determined in B16/F1 melanoma-bearing C57 mice in this study. Among these four ^{99m}Tc-peptides, ^{99m}Tc(EDDA)-HYNIC-AocNle-CycMSH$_{hex}$ exhibited the highest melanoma uptake (22.3 ± 1.72% ID/g) and tumor to kidney uptake ratio at 2 h post-injection. Overall, the properties of high melanoma uptake and fast urinary clearance of ^{99m}Tc(EDDA)-HYNIC-AocNle-CycMSH$_{hex}$ highlighted its clinical potential as an imaging probe for metastatic melanoma detection in the future.

Acknowledgments

Financial Support: This work was supported in part by the NIH grant NM-INBRE P20RR016480/P20GM103451 and University of New Mexico HSC RAC Award. The image in this article was generated by the Keck-UNM Small Animal Imaging Resource established with funding from the W.M. Keck Foundation and the University of New Mexico Cancer Research and Treatment Center (NIH P30 CA118100).

We thank Drs. Jianquan Yang and Fabio Gallazzi for their technical assistance. This work was supported in part by the NIH grant NM-INBRE P20RR016480/P20GM103451 and University of New Mexico HSC RAC Award. The image in this article was generated by the Keck-UNM Small Animal Imaging Resource established with funding from the W.M. Keck Foundation and the University of New Mexico Cancer Research and Treatment Center (NIH P30 CA118100).

References

1. Miao Y, Gallazzi F, Guo H, Quinn TP. ^{111}In-labeled lactam bridge-cyclized alpha-melanocyte stimulating hormone peptide analogues for melanoma imaging. Bioconjug Chem. 2008; 19:539–547. [PubMed: 18197608]
2. Raposinho PD, Correia JD, Alves S, Botelho MF, Santos AC, Santos I. A ^{99m}Tc(CO)$_3$-labeled pyrazolyl-α-melanocyte-stimulating hormone analog conjugate for melanoma targeting. Nucl Med Biol. 2008; 35:91–99. [PubMed: 18158948]
3. Guo H, Shenoy N, Gershman BM, Yang J, Sklar LA, Miao Y. Metastatic melanoma imaging with an ^{111}In-labeled lactam bridge-cyclized alpha-melanocyte-stimulating hormone peptide. Nucl Med Biol. 2009; 36:267–276. [PubMed: 19324272]
4. Guo H, Yang J, Gallazzi F, Prossnitz ER, Sklar LA, Miao Y. Effect of DOTA position on melanoma targeting and pharmacokinetic properties of ^{111}In-labeled lactam bridge-cyclized α-melanocyte stimulating hormone peptide. Bioconjug Chem. 2009; 20:2162–2168. [PubMed: 19817405]
5. Raposinho PD, Xavier C, Correia JD, Falcao S, Gomes P, Santos I. Melanoma targeting with alpha-melanocyte stimulating hormone analogs labeled with fac-[^{99m}Tc(CO)$_3$]$^+$: effect of cyclization on tumor-seeking properties. J Biol Inorg Chem. 2008; 13:449–459. [PubMed: 18183429]
6. Guo H, Yang J, Shenoy N, Miao Y. Gallium-67-labeled lactam bridge-cyclized alpha-melanocyte stimulating hormone peptide for primary and metastatic melanoma imaging. Bioconjug Chem. 2009; 20:2356–2363. [PubMed: 19919057]
7. Guo H, Yang J, Gallazzi F, Miao Y. Reduction of the ring size of radiolabeled lactam bridge-cyclized alpha-MSH peptide resulting in enhanced melanoma uptake. J Nucl Med. 2010; 51:418–426. [PubMed: 20150256]
8. Morais M, Oliveira BL, Correia JD, Oliveira MC, Jiménez MA, Santos I, Raposinho PD. Influence of the bifunctional chelator on the pharmacokinetic properties of ^{99m}Tc(CO)$_3$-labeled cyclic α-melanocyte stimulating hormone analog. J Med Chem. 2013; 56:1961–1973. [PubMed: 23414214]
9. Guo H, Yang J, Gallazzi F, Miao Y. Effects of the amino acid linkers on melanoma-targeting and pharmacokinetic properties of Indium-111-labeled lactam bridge-cyclized α-MSH peptides. J Nucl Med. 2011; 52:608–616. [PubMed: 21421725]

10. Guo H, Miao Y. Cu-64-labeled lactam bridge-cyclized alpha-MSH peptides for PET imaging of melanoma. Mol Pharm. 2012; 9:2322–2330. [PubMed: 22780870]
11. Guo H, Gallazzi F, Miao Y. Ga-67-labeled lactam bridge-cyclized alpha-MSH peptides with enhanced melanoma uptake and reduced renal uptake. Bioconjug Chem. 2012; 23:1341–1348. [PubMed: 22621181]
12. Guo H, Gallazzi F, Miao Y. Design and evaluation of new Tc-99m-labeled lactam bridge-cyclized alpha-MSH peptides for melanoma imaging. Mol Pharm. 2013; 10:1400–1408. [PubMed: 23418722]
13. Hoffman TJ, Gali H, Smith CJ, Sieckman GL, Hayes DL, Owen NK, Volkert WA. Novel series of ^{111}In-labeled bombesin analogs as potential radiopharmaceuticals for specific targeting of gastrin-releasing peptide receptors expressed on human prostate cancer cells. J Nucl Med. 2003; 44:823–831. [PubMed: 12732685]
14. Garayoa EG, Schweinsberg C, Maes V, Brans L, Blauenstein P, Tourwe DA, Schibli R, Schbiger PA. Influence of the molecular charge on the biodistribution of bombesin analogues labeled with the [^{99m}Tc(CO)$_3$]-core. Bioconjug Chem. 2008; 19:2409–2416. [PubMed: 18998719]
15. Fragogeorgi EA, Zikos C, Gourni E, Bouziotis P, Paravatou-Petsotas M, Loudos G, Mitsokapas N, Xanthopoulos S, Mavri-Vavayanni M, Livaniou E, Varvarigou AD, Archimandritis SC. Spacer site modifications for the improvement of the *in vitro* and *in vivo* binding properties of ^{99m}Tc-N$_3$S-X-Bombesin[2–14] derivatives. Bioconjug Chem. 2009; 20:856–867. [PubMed: 19344122]
16. Garrison JC, Rold TL, Sieckman GL, Naz F, Sublett SV, Figueroa SD, Volkert WA, Hoffman TJ. Evaluation of the pharmacokinetic effects of various linking group using the ^{111}In-DOTA-X-BBN(7–14)NH$_2$ structural paradigm in a prostate cancer model. Bioconjug Chem. 2008; 19:1803–1812. [PubMed: 18712899]
17. Parry JJ, Kelly TS, Andrews R, Rogers BE. In vitro and in vivo evaluation of ^{64}Cu-labeled DOTA-Linker-Bombesin(7–14) analogues containing different amino acid linker moieties. Bioconjug Chem. 2007; 18:1110–1117. [PubMed: 17503761]
18. Liu S, He Z, Hsieh WY, Kim YS, Jiang Y. Impact of PKM linkers on biodistribution charateristics of the ^{99m}Tc-labeled cyclic RGDfK dimer. Bioconjug Chem. 2006; 17:1499–1507. [PubMed: 17105229]
19. Shi J, Wang L, Kim YS, Zhai S, Liu Z, Chen X, Liu S. Improving tumor uptake and excretion kinetics of ^{99m}Tc-labeled cyclic arginine-glycine-aspartic (RGD) dimers with triglycine linkers. J Med Chem. 2008; 51:7980–7990. [PubMed: 19049428]
20. Wang L, Shi J, Kim YS, Zhai S, Jia B, Zhao H, Liu Z, Wang F, Chen X, Liu S. Improving tumor-targeting capability and pharmacokinetics of ^{99m}Tc-labeled cyclic RGD dimers with PEG$_4$ linkers. Mol Pharm. 2009; 6:231–245. [PubMed: 19067525]
21. Shi J, Kim YS, Zhai S, Liu Z, Chen X, Liu S. Improving tumor uptake and pharmacokinetics of ^{64}Cu-labeled cyclic RGD peptide dimers with Gly$_3$ and PEG$_4$ linkers. Bioconjug Chem. 2009; 20:750–759. [PubMed: 19320477]
22. Miao Y, Benwell k, Quinn TP. ^{99m}Tc and ^{111}In labeled alpha-melanocyte stimulating hormone peptides as imaging probes for primary and pulmonary metastatic melanoma detection. J Nucl Med. 2007; 48:73–80. [PubMed: 17204701]
23. Kasten BB, Ma X, Liu H, Hayes TR, Barnes CL, Qi S, Cheng K, Bottorff SC, Slocumb WS, Wang J, Cheng Z, Benny PD. Clickable, hydrophilic ligand for *fac*-[M^{I}(CO)$_3$]$^+$ (M = Re/^{99m}Tc) applied in an *S*-functionalized α-MSH peptide. Bioconjug Chem. 2014; 25:579–592. [PubMed: 24568284]
24. Jiang H, Kasten BB, Liu H, Qi S, Liu Y, Tian M, Barnes CL, Zhang H, Cheng Z, Benny PD. Novel, cysteine-modified chelation strategy for the incorporation of [M^{I}(CO)$_3$]$^+$ (M = Re/^{99m}Tc) in an α-MSH peptide. Bioconjug Chem. 2012; 23:2300–2312. [PubMed: 23110503]

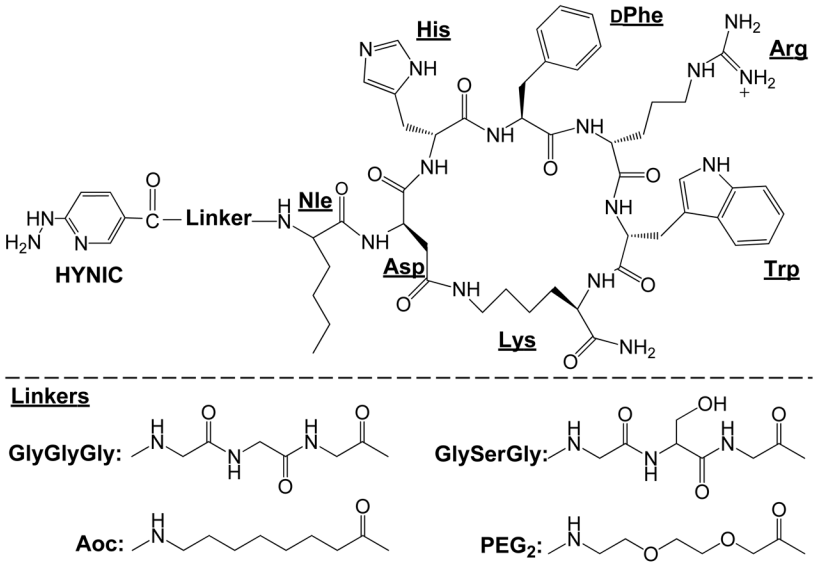

Figure 1.
Schematic structures of HYNIC-Linker-Nle-CycMSH$_{hex}$.

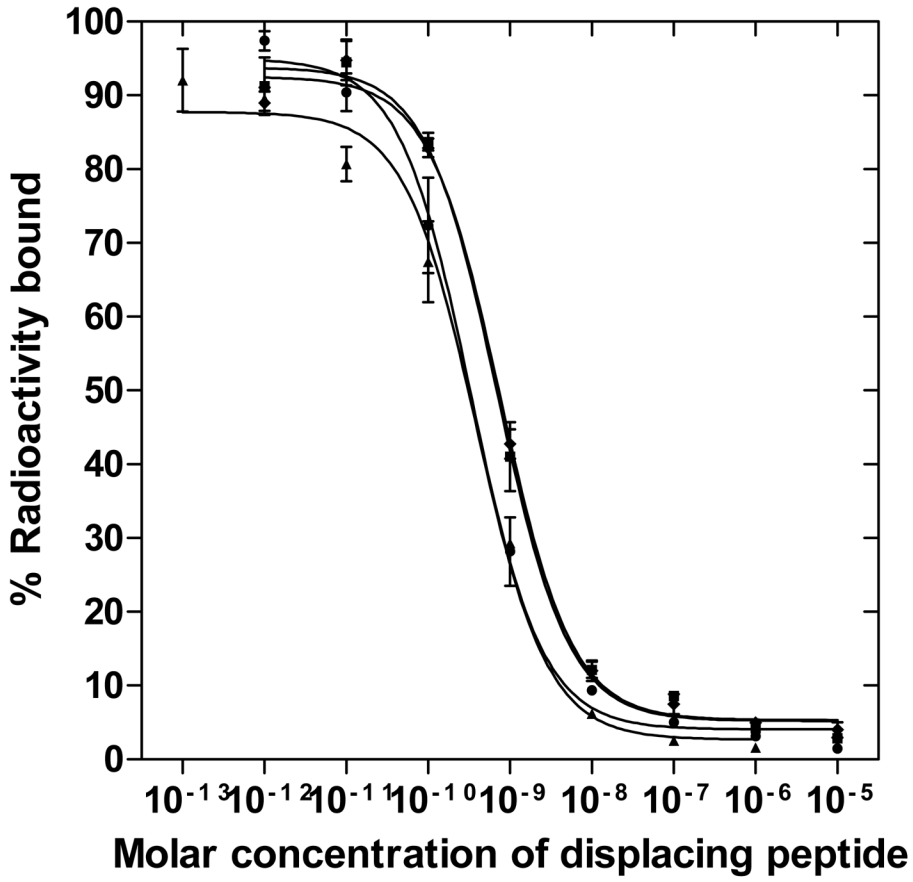

Figure 2.

The *in vitro* competitive binding curve of Hynic-PEG_2Nle-$CycMSH_{hex}$ (●, IC_{50} = 0.3 ± 0.06 nM), Hynic-AocNle-$CycMSH_{hex}$ (▲, IC_{50} = 0.4 ± 0.08 nM), Hynic-GGGNle-$CycMSH_{hex}$ (■, IC_{50} = 0.7 ± 0.1 nM) and Hynic-GSGNle-$CycMSH_{hex}$ (◆, IC_{50} = 0.8 ± 0.09 nM) in B16/F1 murine melanoma cells.

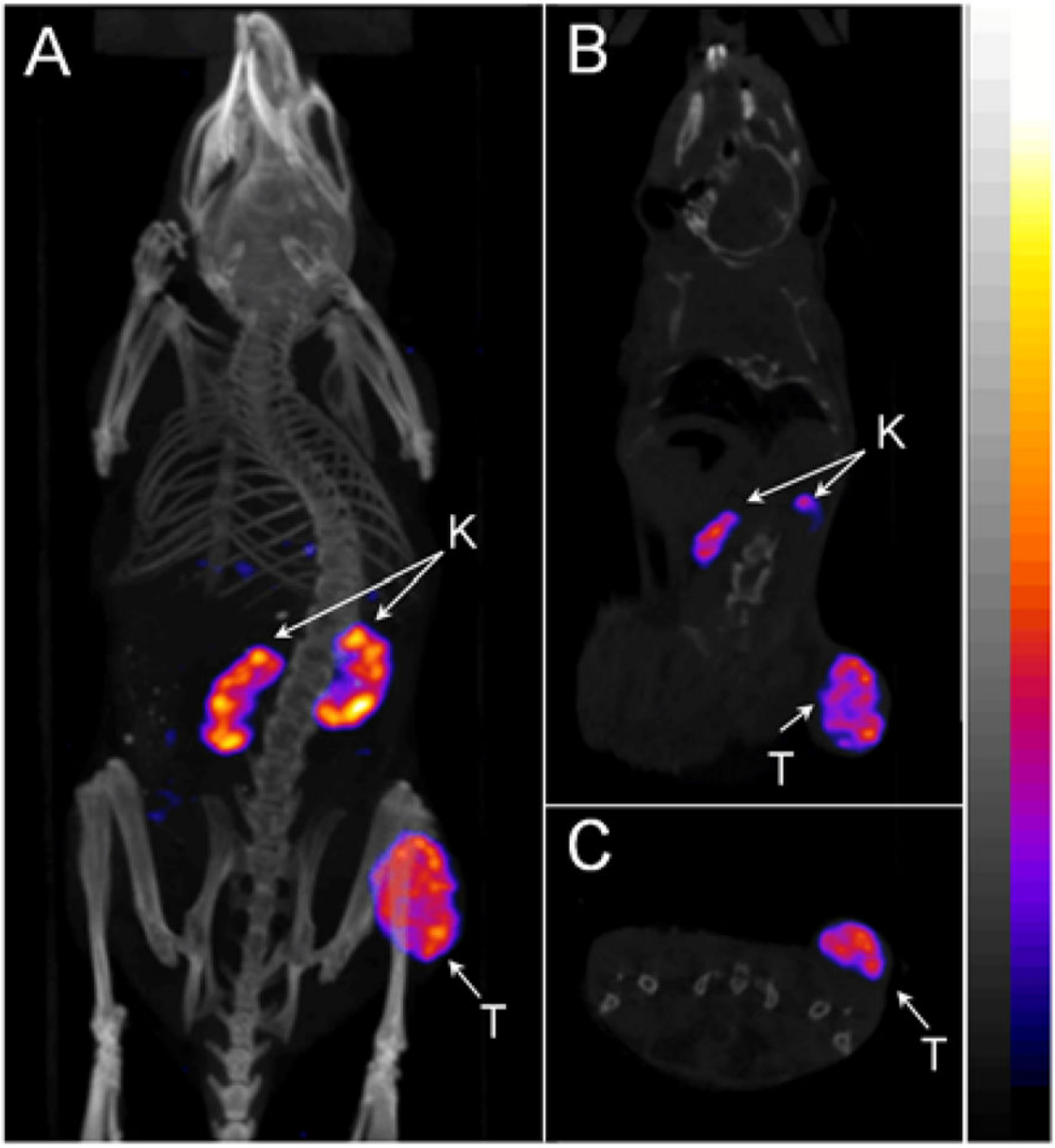

Figure 3.

Representative whole-body (A), coronal (B) and transversal (C) SPECT/CT images of ^{99m}Tc(EDDA)-HYNIC-AocNle-CycMSH$_{hex}$ in a B16/F1 melanoma-bearing C57 mouse at 2 h post-injection. The tumor lesions (T) and kidneys (K) were highlighted with arrows on the images.

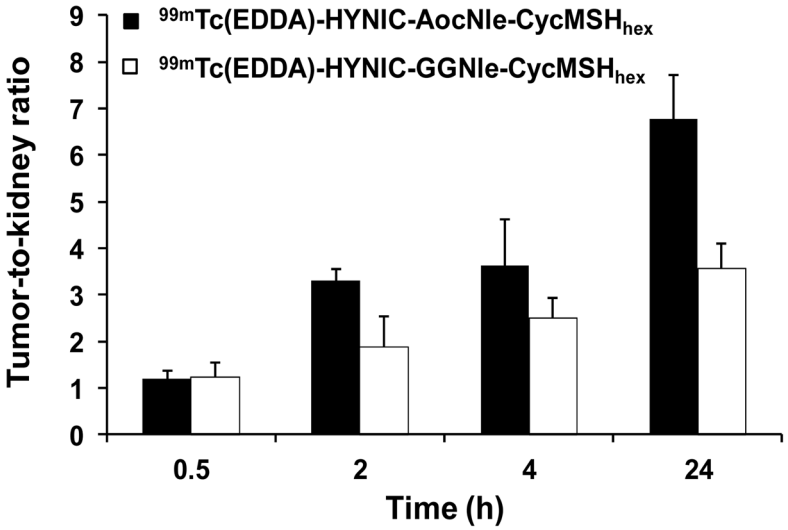

Figure 4.

Comparison in Tumor-to-kidney ratios between ^{99m}Tc(EDDA)-HYNIC-GGNle-CycMSH$_{hex}$ and ^{99m}Tc(EDDA)-HYNIC-AocNle-CycMSH$_{hex}$ at 2, 4 and 24 h post-injection. Data of ^{99m}Tc(EDDA)-HYNIC-GGNle-CycMSH$_{hex}$ were cited from reference 12 for comparison.

Table 1

IC_{50} values and molecular weights (MW) of HYNIC-GGNle-CycMSH$_{hex}$, HYNIC-GGGNle-CycMSH$_{hex}$, HYNIC-GSGNle-CycMSH$_{hex}$, HYNIC-PEG$_2$Nle-CycMSH$_{hex}$, HYNIC-AocNle-CycMSH$_{hex}$ peptides.

Peptide	IC_{50} (nM)	Calculated MW	Measured MW
HYNIC-GGNle-CycMSH$_{hex}$ *	0.6 ± 0.04	1232.4	1232.8
HYNIC-GGGNle-CycMSH$_{hex}$	0.7 ± 0.1	1288.0	1288.2
HYNIC-GSGNle-CycMSH$_{hex}$	0.8 ± 0.09	1318.0	1318.9
HYNIC-PEG$_2$Nle-CycMSH$_{hex}$	0.3 ± 0.06	1262.0	1261.8
HYNIC-AocNle-CycMSH$_{hex}$	0.4 ± 0.08	1257.0	1257.3

* Data of HYNIC-GGNle-CycMSH$_{hex}$ were cited from Ref. 12 for comparison.

Table 2

Biodistribution comparison among ^{99m}Tc(EDDA)-HYNIC-GGGNle-CycMSH$_{hex}$ {GGG}, ^{99m}Tc(EDDA)-HYNIC-GSGNle-CycMSH$_{hex}$ {GSG}, ^{99m}Tc(EDDA)-HYNIC-PEG$_2$Nle-CycMSH$_{hex}$ {PEG$_2$} and ^{99m}Tc(EDDA)-HYNIC-AocNle-CycMSH$_{hex}$ {Aoc}in B16/F1 melanoma-bearing C57 mice at 2 h post-injection. The data were presented as percent injected dose/gram or as percent injected dose (Mean ± SD, n=5).

Tissues	GGG	GSG	PEG$_2$	Aoc
	Percent injected dose/gram (%ID/g)			
Tumor	9.78 ± 3.40	7.41 ± 4.26	14.32 ± 2.82	22.3 ± 1.72
Brain	0.05 ± 0.03	0.07 ± 0.11	0.03 ± 0.02	0.04 ± 0.04
Blood	0.07 ± 0.01	0.08 ± 0.06	0.39 ± 0.07	0.28 ± 0.01
Heart	0.04 ± 0.03	0.06 ± 0.02	0.08 ± 0.03	0.20 ± 0.10
Lung	0.18 ± 0.12	0.15 ± 0.05	0.27 ± 0.12	0.38 ± 0.19
Liver	0.26 ± 0.03	0.23 ± 0.01	0.33 ± 0.03	0.81 ± 0.03
Spleen	0.16 ± 0.09	0.08 ± 0.02	0.11 ± 0.08	0.24 ± 0.00
Stomach	0.43 ± 0.27	0.48 ± 0.39	0.43 ± 0.05	0.70 ± 0.36
Kidneys	5.09 ± 2.19	3.90 ± 1.01	5.79 ± 1.79	6.52 ± 1.04
Muscle	0.03 ± 0.03	0.05 ± 0.02	0.03 ± 0.01	0.06 ± 0.05
Pancreas	0.02 ± 0.01	0.02 ± 0.02	0.08 ± 0.06	0.09 ± 0.00
Bone	0.08 ± 0.06	0.12 ± 0.13	0.29 ± 0.14	0.27 ± 0.10
Skin	0.31 ± 0.10	0.22 ± 0.06	0.49 ± 0.07	0.43 ± 0.11
	Percent injected dose (%ID)			
Intestines	0.52 ± 0.09	0.72 ± 0.27	0.99 ± 0.55	1.85 ± 0.51
Urine	93.90 ± 1.47	95.25 ± 0.52	93.19 ± 1.91	88.46 ± 2.23
	Uptake ratio of tumor/normal tissue			
Tumor/liver	37.26	32.26	43.14	27.51
Tumor/kidney	1.92	1.90	2.48	3.42
Tumor/lung	54.44	50.07	53.72	57.99
Tumor/muscle	351.42	146.90	465.25	378.94
Tumor/blood	147.62	98.05	36.80	79.79
Tumor/skin	31.75	34.01	29.40	52.23

Table 3

Biodistribution of ^{99m}Tc(EDDA)-HYNIC-AocNle-CycMSH$_{hex}$ in B16/F1 melanoma-bearing C57 mice. The data were presented as percent injected dose/gram or as percent injected dose (Mean ± SD, n=5)

Tissues	0.5 h	2 h[#]	4 h	24 h	2-h NDP blockade	2-h L-Lys co-injection
			Percent injected dose/gram (%ID/g)			
Tumor	23.44 ± 3.37	22.8 ± 1.71	22.17 ± 5.93	7.13 ± 0.99	1.26 ± 0.59*	25.85 ± 6.8
Brain	0.17 ± 0.07	0.05 ± 0.03	0.02 ± 0.02	0.01 ± 0.01	0.03 ± 0.01	0.03 ± 0.01
Blood	2.98 ± 1.77	0.40 ± 0.14	0.30 ± 0.14	0.09 ± 0.03	0.82 ± 0.15	0.18 ± 0.13
Heart	1.75 ± 0.31	0.23 ± 0.08	0.13 ± 0.09	0.07 ± 0.02	0.32 ± 0.09	0.14 ± 0.01
Lung	4.06 ± 1.60	0.52 ± 0.20	0.50 ± 0.19	0.14 ± 0.02	0.91 ± 0.06	0.59 ± 0.06
Liver	3.19 ± 0.39	1.09 ± 0.33	1.26 ± 0.60	0.36 ± 0.01	1.22 ± 0.12	1.22 ± 0.15
Spleen	0.94 ± 0.72	0.30 ± 0.13	0.32 ± 0.13	0.05 ± 0.04	0.17 ± 0.11	0.22 ± 0.09
Stomach	2.52 ± 0.22	1.07 ± 0.10	0.73 ± 0.21	0.11 ± 0.02	0.56 ± 0.10	0.97 ± 0.36
Kidneys	19.65 ± 7.36	6.92 ± 1.40	6.10 ± 0.72	1.05 ± 0.07	6.05 ± 1.13	4.64 ± 0.48*
Muscle	0.43 ± 0.14	0.04 ± 0.03	0.04 ± 0.03	0.02 ± 0.01	0.06 ± 0.05	0.07 ± 0.06
Pancreas	0.97 ± 0.40	0.19 ± 0.14	0.44 ± 0.64	0.06 ± 0.03	0.31 ± 0.10	0.06 ± 0.02
Bone	1.09 ± 0.28	0.15 ± 0.09	0.19 ± 0.15	0.12 ± 0.07	0.30 ± 0.08	0.33 ± 0.30
Skin	3.62 ± 0.35	0.46 ± 0.10	0.37 ± 0.11	0.15 ± 0.05	0.45 ± 0.06	0.54 ± 0.10
			Percent injected dose (%ID)			
Intestines	2.43 ± 0.31	1.85 ± 0.51	3.43 ± 0.76	0.32 ± 0.09	1.85 ± 0.42	1.64 ± 0.40
Urine	60.22 ± 4.46	88.46 ± 2.23	84.47 ± 4.80	96.84 ± 1.17	91.29 ± 0.70	88.11 ± 1.90
			Uptake ratio of tumor/normal tissue			
Tumor/liver	7.34	20.86	17.62	20.05	1.03	21.19
Tumor/kidney	1.19	3.29	3.63	6.78	0.21	5.57
Tumor/lung	5.78	43.77	44.51	52.05	1.39	44.16
Tumor/muscle	54.62	527.80	502.79	450.68	21.12	392.26
Tumor/blood	7.87	57.59	74.61	82.89	1.54	139.85
Tumor/skin	6.47	49.13	59.92	47.99	2.82	47.44

[#]2 h Data were cited from Table 2 for comparison;

* $p<0.05$ for determining significance of differences in tumor and kidney uptake between ^{99m}Tc(EDDA)-HYNIC-AocNle-CycMSH$_{hex}$ with or without peptide blockade at 2 h post-injection.